

Elevated Prx1 Provides Resistance to Docetaxel, But Is Not Associated with Predictive Significance in Lung Cancer

Ki Eun Hwang, M.D.¹, Chul Park, M.D.¹, Chang Hwan Seol, M.D.¹, Yu Ri Hwang, M.D.¹, June Seong Hwang, M.D.¹, Jae Wan Jung, M.D.¹, Keum Ha Choi, M.D.², Eun Taik Jeong, M.D., Ph.D.¹ and Hak Ryul Kim, M.D., Ph.D.¹

¹Department of Internal Medicine, Institute of Wonkwang Medical Science, ²Department of Pathology, Wonkwang University School of Medicine, Iksan, Korea

Background: This study was conducted in order to elucidate the effects of docetaxel on the growth of peroxiredoxin 1 (Prx1) knockdown A549 xenograft tumors and further tested the role of Prx1 as a predictor for how a patient would respond to docetaxel treatment.

Methods: Effects of docetaxel on the growth of scrambled- and shPrx1-infected A549 xenograft tumors in nude mice were measured. Moreover, immunohistochemical expression of Prx1 was evaluated in paraffin-embedded tissues from 24 non-small cell lung cancer patients who had received docetaxel-cisplatin regimens as a first-line treatment.

Results: Docetaxel treatment in Prx1 knockdown xenograft tumor resulted in reduced tumors growth compared with other groups. Prx1 knockdown increased the production of cleaved caspases-8 and -9 in the control itself compared to scramble tumors. Moreover, docetaxel treatment in Prx1 knockdown tissue led to an increased protein band. Phosphorylated Akt was found in Prx1 scramble tissues. Phosphorylated FOXO1 was detected in the docetaxel treatment group. On the other hand, Prx1 knockdown completely suppressed the Akt-FOXO1 axis. The median progression-free survival (PFS) of patients with low Prx1 expression was 7 months (95% confidence interval [CI], 6.0–7.7), whereas the median progression-free survival of patients with high Prx1 expression was 4 months (95% CI, 4.0–5.0). However, high Prx1 expression was not associated with decreased PFS ($p=0.114$).

Conclusion: Our findings suggest that elevated Prx1 provides resistance to docetaxel treatment through suppression of FOXO1-induced apoptosis in A549 xenograft tumors, but may not be related with the predictive significance for response to docetaxel treatment.

Keywords: PRDX1 Protein, Human; Docetaxel; Lung Neoplasms

Address for correspondence: Hak Ryul Kim, M.D., Ph.D.

Department of Internal Medicine, Institute of Wonkwang Medical Science, Wonkwang University School of Medicine, 460 Iksan-daero, Iksan 570-749, Korea

Phone: 82-63-859-2583, **Fax:** 82-63-855-2025, **E-mail:** kshryj@wonkwang.ac.kr

Received: Apr. 17, 2013

Revised: May 10, 2013

Accepted: May 27, 2013

©It is identical to the Creative Commons Attribution Non-Commercial License (<http://creativecommons.org/licenses/by-nc/3.0/>).

Copyright © 2013 The Korean Academy of Tuberculosis and Respiratory Diseases. All rights reserved.

Introduction

Lung cancer is the leading cause of cancer-related deaths worldwide¹. Although chemotherapy constitutes a major part of the treatment program for patients with inoperable lung cancer, improvements in treatment efficacy, even with newly developed anticancer agents, have proven unsatisfactory, to date². The development of drug resistance to these anticancer agents represents a major obstacle that needs to be overcome in order to improve the overall response to chemotherapy and the survival rate of lung cancer patients. To guide clinicians in selecting treatment options for patients with a high risk of relapse, reliable markers predictive of recurrence and poor clinical outcomes are desirable.

Docetaxel is one of the most active anticancer agents in the treatment of non-small cell lung cancer (NSCLC) and many other malignancies^{3,4}. Docetaxel is a microtubulin active drug that causes cancer cells to arrest at the G2-M cell cycle transition and ultimately to undergo apoptosis⁵. Although the anti-mitotic mechanisms of docetaxel are not fully understood, many studies have shown that docetaxel induces phosphorylation of anti-apoptotic Bcl-2, activation of mitogen-activated protein kinase, induction of pro-apoptotic cytokine genes, including the Fas/CD95 ligand and apoptosis-related proteins such as p53, p21/WAF-1, Bax, and certain caspases⁶⁻¹¹. Iwao-Koizumi et al.¹² have reported that both gene expression patterns observed in breast cancer patients and *in vitro* transfection findings suggest that redox genes, such as those encoding peroxiredoxins, thioredoxins, and glutathione-S-transferase, play a major role in docetaxel resistance.

Peroxiredoxin 1 (Prx1) is an important member of the redox-regulating peroxiredoxin protein family whose level is frequently elevated in several human cancers¹³⁻¹⁶, including lung cancer¹⁷⁻¹⁹. Accumulating evidence suggests that Prx1 is capable of promoting an aggressive survival phenotype of cancer cells and increasing their resistance to treatment. Elevated Prx1 expression has been correlated with resistance to docetaxel in breast cancer cells. In contrast, down-regulation of Prx1 has been shown to sensitize lung and intestinal cancer cells to radiation and to reduce metastasis²⁰. Recent retrospective immunohistochemical studies have shown that elevated Prx1 is an independent prognostic factor for poor clinical outcome in lung cancer^{21,22}. These studies suggest the potential of Prx1 as a novel prognostic and therapeutic target. However, the effects of Prx1 expression in lung tumors, their influence on cancer therapy, and the regulatory basis for their expression in lung cancer are not clearly understood.

In the present study, we examined the effects of docetaxel on the growth of Prx1 knockdown A549 xenograft tumors, and further tested the role of Prx1 in predicting response to docetaxel treatment.

Materials and Methods

1. Materials

Docetaxel (Taxotere), kindly provided by Aventis Pharma S.A. (Paris, France), was stored as a 100 mM solution in absolute ethanol at -80°C and diluted with a medium before use. The following primary antibodies were used: caspase-8, -9 (Santa Cruz Biotechnology, Santa Cruz, CA, USA); serine/threonine protein kinase (Akt), phospho-Akt, phospho-FOXO1, glyceraldehyde-3-phosphate dehydrogenase (Cell Signaling Technology, Beverly, MA, USA); and Prx1 (Lab Frontier, Seoul, Korea). Anti-rabbit IgG-conjugated horseradish peroxidase (HRP) antibodies and enhanced chemiluminescent (ECL) kit were purchased from Amersham Pharmacia Biotech (Buckinghamshire, UK).

2. Prx1 knockdown by short hairpin RNA (shRNA) in A549 cells

NCI-A549 human lung cancer cells were obtained from the Korean Cell Line Bank (Seoul, Korea) and subjected to Prx1 knockdown. The pSilencer 5.1 system (Ambion, Austin, TX, USA) was used for the expression of Prx1-targeted shRNA. Sense and antisense oligonucleotide sequences targeting human Prx1, as well as a scrambled control, were described by Chhipa et al.²³. The specificity of both shRNA sequences and the scrambled sequences was confirmed by searching the genome database (BLAST). Oligonucleotides were annealed and cloned into the pSilencer vector. Phoenix packaging cells were transfected with either Prx1-shRNA or scrambled-shRNA expression vector by using Lipofectamine 2000 reagent (Invitrogen, Carlsbad, CA, USA). The culture supernatants were collected 48 hours after transfection and filtered. A549 cells were then infected with either Prx1-shRNA or scrambled-shRNA viral preparation in the presence of 4 $\mu\text{g}/\text{mL}$ polybrene (Sigma, St. Louis, MO, USA). Cells expressing scrambled-shRNA or Prx1-shRNA constructs were designated as control or knockdown, respectively.

3. Tumor xenograft studies in nude mice

Five- to six-week-old BALB/c athymic nude mice (Charles River Japan) were housed in cages containing HEPA-filtered air (12-hour light/dark cycle) and had *ad libitum* access to food and autoclaved water. A549 cells (2×10^6 scrambled-infected cells in groups 1 and 2, or 2×10^6 shPrx1-infected cells in groups 3 and 4) were injected subcutaneously (s.c.) into both hind legs of each mouse. Mice were randomly assigned to 4 experimental groups of 7 animals each when implanted tumors reached a volume of 90–130 mm^3 . Mice in groups 1 and 3 received human IgG treatment and they were designated as controls for groups 2 and 4, respectively. Mice in groups 2 and

4 received docetaxel treatment at 20 mg/kg, intraperitoneally (i.p.), once a week. The length (L) and width (W) of the tumor mass were measured 3 times per week. Tumor volume was estimated using the formula: $\text{volume} = L \times W^2 / 2$. All procedures were carried out in accordance with our institutional animal care and use policies.

4. Western blotting

Cells were harvested and lysed using the radioimmunoprecipitation assay buffer (50 mM Tris-Cl [pH, 7.4], 1% NP40, 150 mM NaCl, 1 mM EDTA, 1 mM phenylmethylsulfonyl fluoride, 1 $\mu\text{g}/\text{mL}$ each of aprotinin and leupeptin, and 1 mM Na_3VO_4). After centrifugation at 12,000 $\times g$ for 30 minutes, the supernatant was collected, and the protein concentration was determined by the Lowry method²¹. Equal amounts of protein were separated on 12% sodium dodecyl sulfate-polyacrylamide gel electrophoresis gels under reduced conditions and subsequently transferred to nitrocellulose membranes. Membranes were blocked in 5% skim milk in TBS-T (25 mM Tris [pH, 7.6], 138 mM NaCl, and 0.05% Tween-20) for 1 hour and probed with primary antibodies (at 1:1,000–1:5,000 dilution). After a series of washes, the membranes were further incubated with secondary antibody (at 1:2,000–1:10,000 dilution) conjugated to HRP. Detection of the immunoreactive signal was facilitated using an ECL detection system (Amersham Co.).

5. Reverse transcription polymerase chain reaction (RT-PCR) analysis

The efficiency of shRNA transfection was verified using RT-PCR for TARIL and FasL. After extracting total RNA from the cells by using Trizol (Invitrogen) according to the manufacturer's protocol, single-stranded cDNA was synthesized using RNA as the template. PCR with Taq DNA polymerase (Takara, Takara Shuzo, Kyoto, Japan) was then performed for 25 cycles using the following protocol: 95°C for 10 minutes, 95°C for 1 minute, 57°C for 1 minute, and 72°C for 1 minute. The sequences of primers used for PCR amplification were as follows: TRAIL (forward, 5'-CAA CTC CGT CAG CTC GTT AGA AAG-3'; reverse, 5'-TTA GAC CAA CAA CTA TTT CTA GCA CT-3'); FasL (forward, 5'-GGA TTG GGC CTG GGG ATG TTT CA-3'; reverse, 5'-TTG TGG CTC AGG GGC AGG TTG TTG-3'); β -actin (forward, 5'-GGC GGC ACC ACC ATG TAC CCT-3'; reverse, 5'-AGG GGC CGG ACT CGT CAT ACT-3').

6. Patient selection

We enrolled 24 consecutive patients with histologically confirmed NSCLC and available tumor material for molecular analysis. Furthermore, these patients were treated with docetaxel-cisplatin regimens as first-line treatment at the Wonkwang University Hospital between January 2009 and

December 2010. The study was conducted using an institutional review board (IRB) approved protocol and written informed consent was received from each patient.

7. Specimen preparation and immunohistochemistry

Tissue specimens obtained from diagnostic or therapeutic procedures were fixed in neutral buffered formalin (10% v/v formalin in water, pH 7.4) and embedded in paraffin wax. Serial sections of 4- μm thickness were cut and mounted on charged glass slides (Superfrost Plus; Fisher Scientific, Pittsburgh, PA, USA). In brief, for Prx1, sections were microwaved twice for 10 minutes in citrate buffer (pH 6.0) for antigen retrieval. The sections were then treated with 3% hydrogen peroxide in methanol to quench the endogenous peroxidase activity followed by incubation with 1% bovine serum albumin to block nonspecific binding. A rabbit polyclonal antibody against Prx1 (Lab Frontier) was used at a dilution of 1:2,000. The avidin-biotin detection method was used on a Ventana Automated System (Ventana Medical Systems, Oro Valley, AZ, USA). An irrelevant rabbit antiserum served as a negative control.

8. Assessment of immunostaining and statistical analysis

Each slide was evaluated for Prx1 immunoreactivity by using a semiquantitative scoring system for both the intensity of the stain and the percentage of positive malignant cells. Prx1 immunoreactivity was observed primarily in the cytosol, although focal nuclear expression of Prx1 was noted in some malignant cells. The intensity of cytosolic Prx1 was coded as follows: 0, lower than the adjacent normal-appearing bronchial epithelium; 1, similar to the adjacent bronchial epithelium; 2, stronger than the adjacent bronchial epithelium. The percentage of cells displaying a stronger staining intensity than the adjacent bronchial epithelium was scored as 1 (0–24% tumor cells stained); 2 (25–49% tumor cells stained); 3 (50–74% tumor cells stained); and 4 (75–100% tumor cells stained). For statistical analysis, the median of this series (25% of malignant cells showing a stronger intensity than adjacent bronchial epithelium) was used as a cutoff value to distinguish tumors with a low (<25%) or high (\geq 25%) level of Prx1 expression. The association between staining index and other categorical factors potentially predictive of prognosis was analyzed using the Pearson's χ^2 test of independence. Median progression-free survival (PFS) was measured from the date of first-line therapy initiation to the first radiographic documentation of disease progression or death. Association between Prx1 and PFS was examined using Cox proportional hazards regression models; we report hazard ratio estimates and their 95% confidence intervals (CIs). Data were analyzed using SPSS version 15 (SPSS Inc., Chicago, IL, USA) and MedCalc version 7.5 (MedCalc

Software, Mariakerke, Belgium). Statistical significance was defined as $p < 0.05$.

Results

1. Prx1 knockdown augments the inhibitory effects of docetaxel on tumor growth

We investigated the effects of docetaxel on the growth of scrambled- and shPrx1-infected A549 xenograft tumors in athymic nude mice. We selected 28 mice with similar tumor volumes (90–130 mm³) and analyzed the effects of docetaxel (at 20 mg/kg, i.p., once per week) on tumor growth in mice bearing scrambled- or shPrx1-infected A549 xenograft tumors. Weekly treatment with 20 mg/kg docetaxel did not result in significant toxicity, including weight loss and mortality, in any of the mice (data not shown). With time, scramble-infected A549 control tumors continued to grow, whereas the growth of shPrx1-infected tumors was significantly inhibited, reaching only 45% of the volume of scrambled-infected control tumors. Moreover, compared with other groups, mice bearing shPrx1-infected tumor xenografts showed significantly reduced tumor volume (290.5±54.3 mm³) following docetaxel treatment

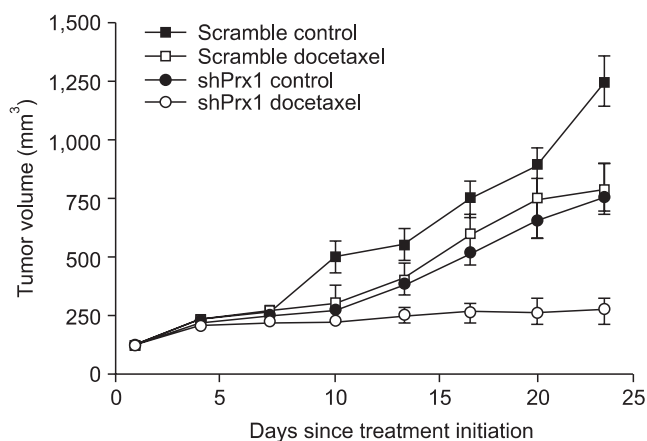


Figure 1. Peroxiredoxin 1 (Prx1) knockdown inhibited the growth of A549 tumors in docetaxel-treated mice. Athymic nude mice were injected subcutaneously with 2×10^6 scrambled- or shPrx1-infected A549 cells (0.2 mL cell suspension) in both hind legs. The mice were randomly divided into 4 groups of 7 animals each: group 1, mice bearing scrambled-infected tumors and receiving human IgG treatment, serving as control for group 2; group 2, mice bearing scrambled-infected tumors and receiving docetaxel treatment at 20 mg/kg, intraperitoneally, once a week; group 3, mice bearing shPrx1-infected tumors and receiving human IgG treatment, serving as control for group 4; and group 4, mice bearing shPrx1-infected tumors and receiving docetaxel treatment at 20 mg/kg, i.p., once a week. Tumors were measured 3 times per week. Tumor volume was estimated using the formula: $\text{volume} = L \times W^2 / 2$. Points, mean of 7 animals; bars, standard deviation.

(Figure 1).

2. Prx1 knockdown suppresses docetaxel-induced apoptosis in A549 xenograft tumors

To test whether the observed growth inhibition was due to a caspase-dependent apoptosis pathway, tissues were evaluated by immunoblotting. Figure 2 shows that Prx1 knockdown increased cleaved caspase-8 in the control and docetaxel treatment groups compared to scramble tumors. Moreover, although cleaved caspase-9 was not detected in the scramble control group, cleaved caspase-9 was found in shPrx1-infected xenograft tumors. In addition, docetaxel treatment in shPrx1-infected xenograft tumors resulted in increased protein. These findings suggest that Prx1 knockdown suppresses docetaxel-induced apoptosis through a caspase cascade in A549 xeno-

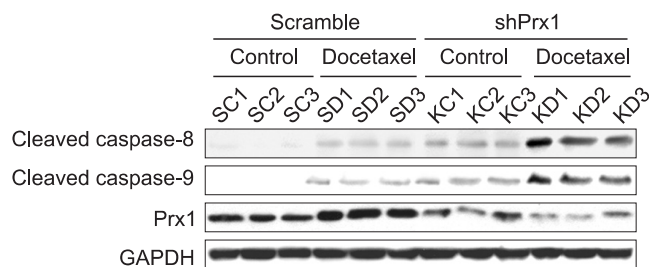


Figure 2. Peroxiredoxin 1 (Prx1) knockdown suppressed docetaxel-induced apoptosis in A549 xenograft tumors. Tumors were analyzed for apoptotic proteins by using immunoblot assay. Cell lysates were subjected to 12% sodium dodecyl sulfate polyacrylamide gel electrophoresis to measure the expression of caspase-8, -9, and Prx1. Glyceraldehyde-3-phosphate dehydrogenase (GAPDH) was used as the protein loading control.

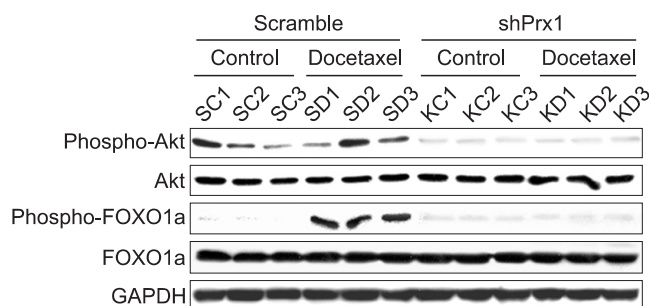


Figure 3. Peroxiredoxin 1 (Prx1) knockdown suppressed docetaxel-induced Akt-FOXO1 pathways in A549 xenograft tumors. Tumors were analyzed for Akt-FOXO1 proteins by using the immunoblot assay. Cell lysates were subjected to 12% sodium dodecyl sulfate polyacrylamide gel electrophoresis to measure the expression of phosphorylated Akt and FOXO1. The same membrane used for anti-phospho antibody staining was stripped and used again with antibody for total Akt. Glyceraldehyde-3-phosphate dehydrogenase (GAPDH) was used as the protein loading control.

graft tumors.

3. Prx1 knockdown suppresses docetaxel-induced Akt-FOXO1 signaling pathways in A549 xenograft tumors

Previously, we demonstrated that phosphorylated Akt and one of its major substrates FOXO1 were increased in a time-dependent manner in scrambled infected A549 cells in vitro. We next tested reproducibility on the A549 xenograft tumors. As shown in Figure 3, phosphorylated Akt was shown

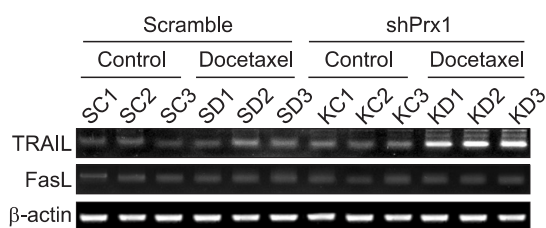


Figure 4. Peroxiredoxin 1 (Prx1) knockdown activated FOXO1 induced TRAIL, but not FasL. Tumors were analyzed for death receptors by using reverse transcription polymerase chain reaction (RT-PCR), which was performed to amplify the TRAIL and FasL genes as described in Materials and Methods. Equal mRNA and protein loading were confirmed using β -actin. RT-PCR data are representative of at least 2 independent experiments.

Table 1. Demographic characteristics of the study population

Baseline characteristic	No. (%)
Gender	
Male	22 (92)
Female	2 (8)
Age, yr	
Median	66.5
Range	38–81
Performance status	
0	9 (38)
1	14 (58)
2	1 (4)
Stage	
IIIa	4 (17)
IIIb	7 (29)
IV	13 (54)
Histology	
Adenocarcinoma	8 (34)
Squamous	14 (58)
Other	2 (8)

in scrambled-infected xenograft tumors as like scrambled-infected cells. In addition, phosphorylated FOXO1 was shown in docetaxel treatment groups in scrambled-infected xenograft tumors. On the other hand, Prx knockdown completely suppressed the Akt-FOXO1 axis in shPrx1-infected xenograft tumors.

4. Effects of Prx1 knockdown on docetaxel-induced death receptors in A549 xenograft tumors

Phosphorylation of FOXO by Akt triggers rapid relocalization of FOXO proteins from the nucleus to the cytoplasm and results in the inhibition of FOXO-dependent transcription of its target genes such as FasL and TRAIL^{25,26}. Therefore, we tested TRAIL and FasL mRNA levels in A549 xenograft tumors by using RT-PCR. Figure 4 shows that docetaxel treat-

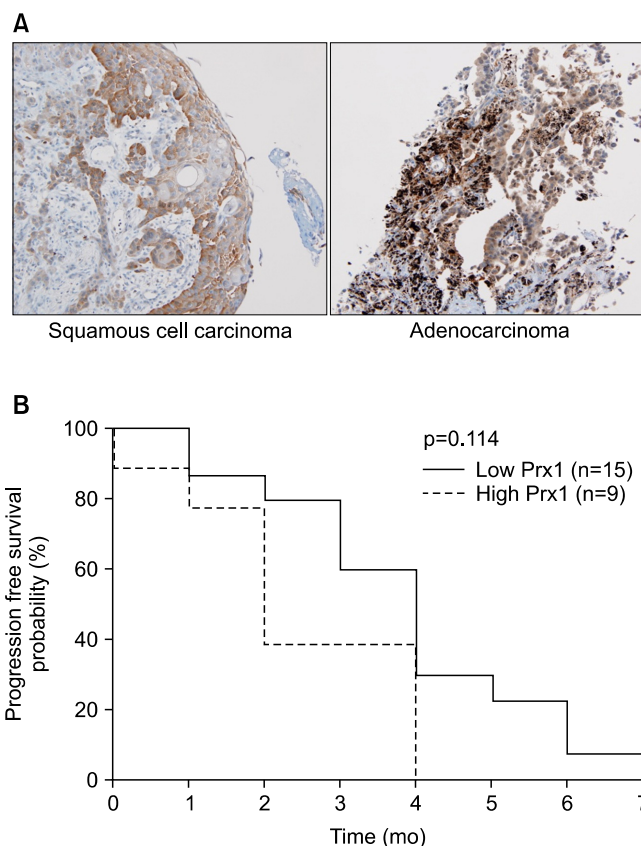


Figure 5. High peroxiredoxin 1 (Prx1) expression did not correlate with progression-free survival (PFS). (A) Immunohistochemical expression of Prx1 in non-small cell lung carcinoma. Typical immunohistological features with high levels of Prx1 expression in squamous cell carcinoma and adenocarcinoma ($\times 200$). The Prx1 staining was primarily present in the cytoplasm of tumor cells. Focal nuclear staining was observed in some malignant cells. (B) PFS determined using Kaplan-Meier survival analysis. The p-value was determined from a log-rank test of the difference.

ment in shPrx1-infected xenograft tumors increased mRNA levels of TRAIL. These findings suggest that Prx1 knockdown suppresses Akt-FOXO1 signaling pathway as activated FOXO1 induced TRAIL, but not FasL.

5. A high level of Prx1 expression does not correlate with reduced PFS

We next examined whether Prx1 expression correlates with PFS for response to docetaxel treatment. Clinical data and representative samples were collected from 24 consecutive patients treated with docetaxel-cisplatin regimens as first-line treatment in our center. Patient characteristics were typical for NSCLC and are summarized in Table 1. A log-rank statistic was used to determine significance. The median PFS of patients with low Prx1 expression was 7 months (95% CI, 6.0–7.7), whereas the median PFS of patients with high Prx1 expression was 4 months (95% CI, 4.0–5.0). However, high Prx1 expression did not correlate with PFS ($p=0.114$) (Figure 5).

Discussion

Improving the efficacy of docetaxel by inhibiting pro-survival pathways or enhancing docetaxel effects on apoptosis has implications for treatment of lung cancer²⁷. We have reported that Prx1 modulates the chemosensitivity of lung cancer cells to docetaxel through suppression of FOXO1-induced apoptosis. In the present study, we show that elevated Prx1 provides resistance to docetaxel treatment through suppression of FOXO1-induced apoptosis in A549 xenograft tumors, but may not be related with predictive significance for response to docetaxel treatment.

Resistance to docetaxel may result from interference with the steps leading to the induction of apoptosis. These include modulation of β -tubulin isoforms²⁸, upregulation of the cell cycle regulatory protein p21²⁹, inhibition of the proapoptotic protein BAD, and upregulation of prosurvival pathways involving Bcl-2 and phosphatidylinositol 3-kinase³⁰. To the best of our knowledge, this is the first study to identify Prx1 as an important mediator of resistance to docetaxel-induced apoptosis in lung cancer. The present studies may provide valuable insights into the basis for sensitivity or resistance of lung cancer to docetaxel.

Prx1 interacts with and modulates the activities of cell survival regulatory proteins to increase radioresistance¹⁸. The Akt pathway may promote tumor cell survival by suppressing cell death induced by a number of apoptotic stimuli, including chemotherapeutic agents. Activation of Akt is a frequently observed phenomenon following treatment with docetaxel^{31,32}. Therefore, activation of Akt by docetaxel may account for desensitization to docetaxel in scrambled-infected A549 xe-

nograft tumors. Many studies have shown that Akt directly phosphorylates FOXO transcription factors^{33,34}, and the mechanisms through which Akt regulates FOXO transcription factors have been previously elucidated³⁵. Phosphorylation of FOXO by Akt triggers rapid relocalization of FOXO proteins from the nucleus to the cytoplasm leading to inhibition of FOXO-dependent transcription of its target genes such as FasL and TRAIL^{26,36,37}. We have found that A549 xenograft tumors express FOXO1, but not other members of the FOXO family (data not shown). We thus examined the effects of docetaxel on phosphorylation of Akt and FOXO1. Our results demonstrated that docetaxel caused an increase in the phosphorylation of both Akt and FOXO1 in scrambled-infected A549 xenograft tumors, whereas Prx1 knockdown suppressed docetaxel-induced phosphorylation of both these proteins. These findings suggest that neutralization of Prx1 modifies the Akt-FOXO1 axis, increasing the death receptor-mediated extrinsic apoptosis pathway and caspase-8 activation.

Although the investigation of Prx1 function in cultured cells and animal systems indicates its cell survival enhancing properties, no research has previously been undertaken to evaluate the prognostic value of Prx1 in lung cancer. We have determined whether the Prx1 expression correlates with PFS for response to docetaxel treatment. However, a higher pretreatment Prx1 level did not correlate with PFS. The main limitation of the present study is that this is a retrospective study with comparatively small size, and further research that examines a larger group of patients is warranted. Another limitation is that since patients were treated with docetaxel-cisplatin regimens, we cannot exclude the possibility of cisplatin-mediated effects.

In summary, our results show that elevated Prx1 provides resistance to docetaxel treatment through suppression of FOXO1-induced apoptosis in A549 xenograft tumors, but may not be related with predictive significance for response to docetaxel treatment. Therefore, Prx1 may be an attractive target in the development of more effective docetaxel-based therapies in lung cancer treatment.

Acknowledgements

This study was supported by a 2011 grant from the Korean Academy of Tuberculosis and Respiratory Diseases.

References

1. Jemal A, Siegel R, Xu J, Ward E. Cancer statistics, 2010. *CA Cancer J Clin* 2010;60:277-300.
2. Rigas JR. Do newer chemotherapeutic agents improve survival in non-small cell lung cancer? *Semin Oncol* 1998;25(3 Suppl 8):5-9.

3. Posner MR. Docetaxel in squamous cell cancer of the head and neck. *Anticancer Drugs* 2001;12 Suppl 1:S21-4.
4. Rowinsky EK. The development and clinical utility of the taxane class of antimicrotubule chemotherapy agents. *Annu Rev Med* 1997;48:353-74.
5. Bhalla KN. Microtubule-targeted anticancer agents and apoptosis. *Oncogene* 2003;22:9075-86.
6. Haldar S, Chintapalli J, Croce CM. Taxol induces bcl-2 phosphorylation and death of prostate cancer cells. *Cancer Res* 1996;56:1253-5.
7. Haldar S, Basu A, Croce CM. Bcl2 is the guardian of microtubule integrity. *Cancer Res* 1997;57:229-33.
8. Lee LF, Li G, Templeton DJ, Ting JP. Paclitaxel (Taxol)-induced gene expression and cell death are both mediated by the activation of c-Jun NH2-terminal kinase (JNK/SAPK). *J Biol Chem* 1998;273:28253-60.
9. Amato SE, Swart JM, Berg M, Wanebo HJ, Mehta SR, Chiles TC. Transient stimulation of the c-Jun-NH2-terminal kinase/activator protein 1 pathway and inhibition of extracellular signal-regulated kinase are early effects in paclitaxel-mediated apoptosis in human B lymphoblasts. *Cancer Res* 1998;58:241-7.
10. Mhaidat NM, Zhang XD, Jiang CC, Hersey P. Docetaxel-induced apoptosis of human melanoma is mediated by activation of c-Jun NH2-terminal kinase and inhibited by the mitogen-activated protein kinase extracellular signal-regulated kinase 1/2 pathway. *Clin Cancer Res* 2007;13:1308-14.
11. Mhaidat NM, Wang Y, Kiejda KA, Zhang XD, Hersey P. Docetaxel-induced apoptosis in melanoma cells is dependent on activation of caspase-2. *Mol Cancer Ther* 2007;6:752-61.
12. Iwao-Koizumi K, Matoba R, Ueno N, Kim SJ, Ando A, Miyoshi Y, et al. Prediction of docetaxel response in human breast cancer by gene expression profiling. *J Clin Oncol* 2005;23:422-31.
13. Rhee SG, Kang SW, Chang TS, Jeong W, Kim K. Peroxiredoxin, a novel family of peroxidases. *IUBMB Life* 2001;52:35-41.
14. Yanagawa T, Ishikawa T, Ishii T, Tabuchi K, Iwasa S, Bannai S, et al. Peroxiredoxin I expression in human thyroid tumors. *Cancer Lett* 1999;145:127-32.
15. Yanagawa T, Iwasa S, Ishii T, Tabuchi K, Yusa H, Onizawa K, et al. Peroxiredoxin I expression in oral cancer: a potential new tumor marker. *Cancer Lett* 2000;156:27-35.
16. Noh DY, Ahn SJ, Lee RA, Kim SW, Park IA, Chae HZ. Overexpression of peroxiredoxin in human breast cancer. *Anticancer Res* 2001;21:2085-90.
17. Lehtonen ST, Svensk AM, Soini Y, Paakko P, Hirvikoski P, Kang SW, et al. Peroxiredoxins, a novel protein family in lung cancer. *Int J Cancer* 2004;111:514-21.
18. Kim HJ, Chae HZ, Kim YJ, Kim YH, Hwangs TS, Park EM, et al. Preferential elevation of Prx I and Trx expression in lung cancer cells following hypoxia and in human lung cancer tissues. *Cell Biol Toxicol* 2003;19:285-98.
19. Chang JW, Lee SH, Jeong JY, Chae HZ, Kim YC, Park ZY, et al. Peroxiredoxin-I is an autoimmunogenic tumor antigen in non-small cell lung cancer. *FEBS Lett* 2005;579:2873-7.
20. Chen MF, Keng PC, Shau H, Wu CT, Hu YC, Liao SK, et al. Inhibition of lung tumor growth and augmentation of radiosensitivity by decreasing peroxiredoxin I expression. *Int J Radiat Oncol Biol Phys* 2006;64:581-91.
21. Kim JH, Bogner PN, Ramnath N, Park Y, Yu J, Park YM. Elevated peroxiredoxin 1, but not NF-E2-related factor 2, is an independent prognostic factor for disease recurrence and reduced survival in stage I non-small cell lung cancer. *Clin Cancer Res* 2007;13:3875-82.
22. Kim JH, Bogner PN, Baek SH, Ramnath N, Liang P, Kim HR, et al. Up-regulation of peroxiredoxin 1 in lung cancer and its implication as a prognostic and therapeutic target. *Clin Cancer Res* 2008;14:2326-33.
23. Chhipa RR, Lee KS, Onate S, Wu Y, Ip C. Prx1 enhances androgen receptor function in prostate cancer cells by increasing receptor affinity to dihydrotestosterone. *Mol Cancer Res* 2009;7:1543-52.
24. Lowry OH, Rosebrough NJ, Farr AL, Randall RJ. Protein measurement with the Folin phenol reagent. *J Biol Chem* 1951;193:265-75.
25. Suhara T, Kim HS, Kirshenbaum LA, Walsh K. Suppression of Akt signaling induces Fas ligand expression: involvement of caspase and Jun kinase activation in Akt-mediated Fas ligand regulation. *Mol Cell Biol* 2002;22:680-91.
26. Dijkers PF, Medema RH, Lammers JW, Koenderman L, Coffey PJ. Expression of the pro-apoptotic Bcl-2 family member Bim is regulated by the forkhead transcription factor FKHR-L1. *Curr Biol* 2000;10:1201-4.
27. Tannock IF, de Wit R, Berry WR, Horti J, Pluzanska A, Chi KN, et al. Docetaxel plus prednisone or mitoxantrone plus prednisone for advanced prostate cancer. *N Engl J Med* 2004;351:1502-12.
28. Montgomery RB, Bonham M, Nelson PS, Grim J, Makary E, Vessella R, et al. Estrogen effects on tubulin expression and taxane mediated cytotoxicity in prostate cancer cells. *Prostate* 2005;65:141-50.
29. Yu D, Jing T, Liu B, Yao J, Tan M, McDonnell TJ, et al. Overexpression of ErbB2 blocks Taxol-induced apoptosis by upregulation of p21Cip1, which inhibits p34Cdc2 kinase. *Mol Cell* 1998;2:581-91.
30. Wu JD, Haugk K, Coleman I, Woodke L, Vessella R, Nelson P, et al. Combined *in vivo* effect of A12, a type 1 insulin-like growth factor receptor antibody, and docetaxel against prostate cancer tumors. *Clin Cancer Res* 2006;12(20 Pt 1):6153-60.
31. Xing H, Weng D, Chen G, Tao W, Zhu T, Yang X, et al. Activation of fibronectin/PI-3K/Akt2 leads to chemoresistance to docetaxel by regulating survivin protein expression in ovarian and breast cancer cells. *Cancer Lett* 2008;261:108-19.
32. Kosaka T, Miyajima A, Shirotake S, Suzuki E, Kikuchi E, Oya M. Long-term androgen ablation and docetaxel up-regulate

- phosphorylated Akt in castration resistant prostate cancer. *J Urol* 2011;185:2376-81.
33. Biggs WH 3rd, Meisenhelder J, Hunter T, Cavenee WK, Arden KC. Protein kinase B/Akt-mediated phosphorylation promotes nuclear exclusion of the winged helix transcription factor FKHRL1. *Proc Natl Acad Sci U S A* 1999;96:7421-6.
34. Kops GJ, Burgering BM. Forkhead transcription factors: new insights into protein kinase B (c-akt) signaling. *J Mol Med (Berl)* 1999;77:656-65.
35. Brunet A, Bonni A, Zigmond MJ, Lin MZ, Juo P, Hu LS, et al. Akt promotes cell survival by phosphorylating and inhibiting a Forkhead transcription factor. *Cell* 1999;96:857-68.
36. Modur V, Nagarajan R, Evers BM, Milbrandt J. FOXO proteins regulate tumor necrosis factor-related apoptosis inducing ligand expression. Implications for *PTEN* mutation in prostate cancer. *J Biol Chem* 2002;277:47928-37.
37. Lee YJ, Park MY, Kang YA, Kwon SY, Yoon HI, Lee JH, et al. Enhancement of sensitivity of human lung cancer cell line to TRAIL and gefitinib of IGF-1R blockade. *Tuberc Respir Dis* 2007;63:42-51.